Beina Teng,[1] Patricia Schroder,[2] Janina Müller-Deile,[1] Heiko Schenk,[1] Lynne Staggs,[2] Irini Tossidou,[1] Ivan Dikic,[3] Hermann Haller,[1] and Mario Schiffer[1]

CIN85 Deficiency Prevents Nephrin Endocytosis and Proteinuria in Diabetes

Diabetes 2016;65:3667–3679 | DOI: 10.2337/db16-0081

Diabetic nephropathy (DN) is the major cause of end-stage renal disease worldwide. Podocytes are important for glomerular filtration barrier function and maintenance of size selectivity in protein filtration in the kidney. Podocyte damage is the basis of many glomerular diseases characterized by loss of interdigitating foot processes and decreased expression of components of the slit diaphragm. Nephrin, a podocyte-specific protein, is the main component of the slit diaphragm. Loss of nephrin is observed in human and rodent models of diabetic kidney disease. The long isoform of CIN85 (RukL) is a binding partner of nephrin that mediates nephrin endocytosis via ubiquitination in podocytes. Here we demonstrate that the loss of nephrin expression and the onset of proteinuria in diabetic mice correlate with an increased accumulation of ubiquitinated proteins and expression of CIN85/RukL in podocytes. CIN85/RukL deficiency preserved nephrin surface expression on the slit diaphragm and reduced proteinuria in diabetic mice, whereas overexpression of CIN85 in zebrafish induced severe edema and disruption of the filtration barrier. Thus, CIN85/RukL is involved in endocytosis of nephrin in podocytes under diabetic conditions, causing podocyte depletion and promoting proteinuria. CIN85/RukL expression therefore shows potential to be a novel target for antiproteinuric therapy in diabetes.

Diabetic nephropathy (DN) is a common cause of end-stage renal failure and is epidemic worldwide (1). The clinical hallmark of DN is proteinuria, which is considered to play a central role in the pathogenesis of progressive renal dysfunction. Over the past few decades, mesangial cells and the glomerular basement membrane (GBM) have tended to be the focus of many DN studies. Glomerular changes in DN are characterized by glomerular hypertrophy, mesangial matrix expansion, and GBM thickening. Studies of patients with diabetes and experimental models reveal that the onset albuminuria is most closely associated with podocytopathies such as foot process effacement, podocyte hypertrophy, detachment, apoptosis, and transdifferentiation (2–5). Because the terminally differentiated podocytes are believed to play a critical role in maintaining the integrity of the glomerular filtration barrier, podocyte effacement may contribute to the development of albuminuria. Although structural proteins were initially thought to be the key elements that compose the slit diaphragm, it has become clear that the slit diaphragm protein complex is a highly dynamic functional protein complex and is able to initiate cascades of signaling pathways that affect podocyte function (6). More recent data indicate that podocytes express receptors for many circulating hormones and growth factors, which also suggest that a more complex cross talk between the kidney and other organs affected by diabetes may occur in health and disease (7).

Nephrin is a 180-kDa transmembrane protein predominantly localized to the glomerular slit diaphragm. Its presence is essential for primary structural function of the slit diaphragm (8). Nephrin may also act as a signaling adhesion molecule, triggering phosphorylation and activation of several kinase cascades (9). Nephrin signaling is augmented by its interaction with podocin. During the early stage of human and experimental DN, podocytes lose nephrin expression, become effaced, and detach from the GBM or undergo apoptosis, events that correlate with the emergence of albuminuria (3,10).

[1]Division of Nephrology, Department of Medicine, Hannover Medical School, Hannover, Germany
[2]Mount Desert Island Biological Laboratory, Salisbury Cove, ME
[3]Institute of Biochemistry II, Goethe University Frankfurt, Frankfurt, Germany
Corresponding author: Mario Schiffer, schiffer.mario@mh-hannover.de.

Received 15 January 2016 and accepted 31 July 2016.

See accompanying article, p. 3532.

Regulator of ubiquitous kinase/Cbl-interacting protein of 85 kDa (Ruk/CIN85) is known as an adaptor protein belonging to the CD2AP family, which is involved in clathrin-mediated receptor endocytosis of receptor tyrosine kinases (RTKs) (11,12). In rodents and humans, Ruk/CIN85 is composed of three N-terminal Src homology (SH) domains, followed by one proline-rich domain and a COOH-terminal coiled-coil domain. The presence of these multiple protein-protein binding motifs allows the interaction of Ruk/CIN85 with various signaling molecules and, consequently, functional involvement in many intracellular networks (13). The CIN85 genomic locus gives rise to multiple isoforms, including CIN85-xl, CIN85-l (CIN85/RukL), CIN85-ΔA, CIN85-m, CIN85-s, CIN85-t, and CIN85-h, as a result of alternative splicing and differential promoter usage (14,15). CIN85/RukL was identified as an interaction partner of c-Cbl, an E3 ubiquitin ligase. c-Cbl ubiquitinates many cell surface receptors and, by means of this posttranslational modification, initiates their internalization, endocytic trafficking, and sorting (16,17).

We previously defined CIN85/RukL as a binding partner of nephrin and a mediator of nephrin endocytosis (18). CIN85/RukL binds nephrin through its SH3 domain. The expression of CIN85 is posttranscriptionally regulated via ubiquitination or small ubiquitin-like modifier (SUMO)ylation (19) and is described to regulate ubiquitination and several types of degradative endosomal sorting. So far, most conclusions about the involvement of CIN85/RukL in endocytosis and other trafficking events are based on studies in CD2AP-knockout cells or artificial overexpression studies of this protein. In this study, we first detect a glucose-induced expression induction of endogenous CIN85/RukL and investigate the role of CIN85/RukL in diabetes in vivo in CIN85$^{\Delta ex2}$ mice.

RESEARCH DESIGN AND METHODS

Antibodies

The antibodies used for Western blot analysis, immunoprecipitation, immunofluorescence, and immunohistochemistry were as follows: rabbit anti-nephrin (targeting for the extracellular domain), rabbit anti-CD2AP, rabbit anti-GAPDH (Santa Cruz Biotechnology, Santa Cruz, CA), mouse anti-ubiquitin (Imgenex, San Diego, CA), mouse anti-CIN85 (Upstate), rabbit anti-SUMO-1 (Cell Signaling), guinea pig anti-nephrin (Progen, Heidelberg, Germany), and mouse anti-CIN85 (gift from I.D.). Peroxidase-conjugated donkey anti-rabbit, goat anti-mouse, and unconjugated rabbit IgG were from Santa Cruz Biotechnology. Alexa Fluor 488 goat anti-guinea pig and Alexa Fluor 555 donkey anti-mouse antibodies were from Invitrogen.

Podocyte Culture

Cultivation of conditionally immortalized wild-type, CD2AP$^{-/-}$, and CIN85$^{\Delta ex2}$ murine podocytes was performed as previously described by Mundel and Reiser (20). In brief, to enhance expression of the thermosensitive large T antigen, cells were cultured at 33°C in the presence of 10 units/mL γ-interferon (permissive conditions). To induce differentiation, podocytes were maintained at 37°C for 10–14 days without γ-interferon, leading to degradation of thermosensitive T antigen (nonpermissive conditions). The results for every experimental setup were confirmed in three different clones of wild-type, CD2AP$^{-/-}$, and CIN85$^{\Delta ex2}$ murine podocytes.

Western Blot Analysis

To analyze whole-cell protein lysates from cultured podocytes, they were lysed on ice with radioimmunoprecipitation assay (RIPA) buffer (50 mmol/L Tris [pH 7.5], 150 mmol/L NaCl, 0.5% sodium deoxycholate, 1% Nonidet P-40, and 0.1% SDS) containing protease inhibitors (cOmplete Mini, Roche Applied Science), 1 mmol/L sodium orthovanadate, 50 mmol/L NaF, and 200 ng/mL okadaic acid. The lysates were centrifuged 15 min at 12,000 rpm and 4°C. Protein was quantified using the BCA Protein Assay Kit (Pierce Chemical Co., Thermo Fisher Scientific, Inc.). Samples from the supernatants were separated by 10% SDS-PAGE and transferred to polyvinylidene difluoride membranes (Immobilon-P; Millipore, Bedford, MA). After samples were probed with primary antibodies, antigen-antibody complexes were detected with horseradish peroxidase–labeled anti-rabbit or anti-mouse secondary antibodies and visualized using SuperSignal West Pico Chemiluminescent Substrate (Pierce Chemical Co.) according to the manufacturer's protocol.

Ubiquitination Assay (Immunoprecipitation)

Podocytes were subcultured on plates and differentiated for 14 days. The cells were carefully washed with ice-cold PBS and lysed with 300 μL RIPA buffer (50 mmol/L Tris-HCl [pH 7.5], 150 mmol/L NaCl, 0.5% sodium deoxycholate, 1% Nonidet P-40, and 0.1% SDS) containing protease inhibitor (Roche Applied Science). The lysates were rotated for 60 min at 4°C and centrifuged at 14,000 rpm for 15 min. Agarose-A beads (50 μL; Santa Cruz Biotechnology) and nephrin (5 μL) were added to at least 500 μg of total cell lysate with concentration of 1 μg/μL. The samples were rotated overnight at 4°C. The pellets were washed three times with RIPA buffer and separated by SDS-PAGE.

Endocytosis Assay Using ELISA

Adenovirus-infected human podocytes or murine podocytes were seeded in a 24-well plate coated with poly-L-lysine (1:1 diluted with H_2O). To induce internalization, cells were incubated with 30 mmol/L high glucose or mannitol medium for 2 or 24 h at 37°C. The plates were cooled on ice for 10–15 min. The medium was replaced with DFH medium (1% FCS and 20 mmol/L HEPES in RPMI 1640 medium) containing 1:500 rabbit anti-nephrin antibody. Please note the two DFH solutions differ only slightly in HEPES concentration. The cells were incubated for 60 min at 4°C and then washed three times with cold DFHI medium (1% FCS and 25 mmol/L HEPES in RPMI 1640 medium). The cells were then fixed with 3.7% paraformaldehyde for 15 min, washed twice with PBS, and kept overnight at 4°C. For blocking, 2%

normal goat serum (Jackson ImmunoResearch) in PBS was used for at least 30 min. Cells were washed once with PBS and were incubated in PBS with alkaline phosphatase-coupled anti-rabbit antibody (dilution 1:7,500) for 1 h and washed three times with PBS, with each wash 5–10 min. The cells were then incubated with *p*-nitrophenyl phosphate (N2765; Sigma-Aldrich) by resuspending one tablet in 20 mL of 0.1 mol/L glycine, 1 mmol/L $MgCl_2$, and 1 mmol/L $ZnCl_2$ (pH 10.4) for ~1 h at 37°C or until the solution turned yellow. One aliquot (100 μL) from the reaction was transferred into a well of a 96-well plate, and the extinction was measured at 405 nm in a microplate reader (Tecan).

Immunofluorescence and Histochemistry

For immunofluorescence staining of frozen kidneys, 6-μm sections (Leica CM3050S cryostat; Leica Microsystems, Wetzlar, Germany) were fixed in acetone, or 1.5-μm paraffin sections were deparaffinized, and antigen retrieval was performed by heating in citrate buffer (10 mmol/L sodium citrate, pH 6.0) in a microwave or by digesting with 1 mg/mL trypsin (T7168; Sigma-Aldrich). For immunofluorescence staining, unspecific binding was blocked with 10% donkey serum 30 min at room temperature. Sections were incubated with the primary antibodies as indicated overnight at 4°C, after rinsing with TBS (50 mmol/L Tris and 150 mmol/L NaCl, pH 7.4–7.6). The sections were incubated with fluorescence-conjugated secondary antibody at room temperature for 30 min and mounted with Aqua Poly (Polysciences, Inc.).

The histoimmunochemical staining was performed with the VECTASTAIN ABC Kit and ACE peroxidase substrate kit (Vector Laboratories, Inc.) according to the manufacturer's instructions.

PCR

Total mRNA was isolated from podocytes using an RNA kit (Qiagen, Hilden, Germany) according to the manufacturer's instructions, after which 1 μg RNA was reverse transcribed with random and hexamer primers and T reverse transcriptase (Promega). Primers for detecting mRNA expression of CIN85 full length were described by Buchman et al. (14): CIN85 m1: forward 5′-TTCCGCCAACTTTCACTCTG-3′, and CIN85 mmn: reverse 5′-GGCAGGAAGTCATTTTCCAC-3′. HPRT-1: forward 5′-CAGTCCCAGCGTCGTGATTA-3′ and reverse 5′-AGCAAGTCTTTCAGTCCTGTC-3′ were used as an internal control to correct for small variations in mRNA quality and cDNA synthesis.

Animal Experiments

Ethics Statement

Animal work was conducted according to the guidelines of the American Physiological Society and was approved by the Hannover Medical School Institutional Animal Care and Use Committee and the Animal Welfare Authorities of Lower Saxony (Protocol #11/0545). All efforts were made to minimize the number of animals used and their suffering. The mice received a standard diet with free access to tap water.

Genotyping

Genomic DNA samples from tail biopsy specimens were used. PCR was performed under standard conditions in a Primus Thermocycler (MWG-Biotech AG, Ebersberg, Germany) with the following primer pairs: CIN85 neo forward: 5′- GCTGCTATTGGGCGAAGTG-3′, CIN85 wild-type forward 5′- AGGGAGGATGGAGGCTGGTG-3′, and CIN85 wild-type reverse: 5′- GATGAAGGCAAGTCTATGAGGA-3′.

Streptozocin-Induced Type 1 Diabetic Mice

C57BL/6J wild-type and $CIN85^{\Delta ex2}$ mice (gift from I.D.) were intraperitoneally injected with 50 mg/kg streptozocin (STZ) (Sigma-Aldrich) diluted in 50 mmol/L sodium citrate (Fisher Scientific) buffer (pH 4.5) or with sodium citrate buffer for 5 consecutive days. Glucose levels from tail blood were measured with Glucometer Elite (Bayer, Leverkusen, Germany) every other day. The glucose levels were monitored 4 weeks after injection and then every week until the animals were hyperglycemic for 16 weeks. Animals with glucose levels exceeding 16 mmol/L on two consecutive measurements were regarded as hyperglycemic. The mice were not supplied with insulin during the experiment.

Microalbuminuria and Creatinine Measurement

Urine of each mouse was collected in metabolic cages and was analyzed for albuminuria and creatinine content using commercially available kits (Bethyl Laboratories, Inc. and Exocell, Inc.). The measurements were performed according to the manufacturer's protocol.

Zebrafish Experiments

Zebrafish were mated and embryos housed at 28.5°C in embryo-rearing media (E3). The Nanoject II injection device (Drummond Scientific, Broomall, PA) was used to inject 4.6 nL capped RNA for murine CIN85 and CD2AP diluted 1:1 with injection buffer (20 mmol/L HEPES, 200 mmol/L KCl, and 0.75% phenol red) into one- to four-cell stage fertilized embryos at different concentrations. The capped RNAs were synthesized using mMESSAGE mMACHINE kits (Ambion) according to the manufacturer's protocol. Because capped RNA has a 7-methyl guanosine cap structure at the 5′ end, it mimics most eukaryotic mRNAs found in vivo.

For observation of proteinuria, we used the Tg(*l*-fabp:DBP-EGFP) transgenic zebrafish line as previously described (21,22). Fluorescence of eGFP-labeled vitamin D–binding protein (eGFP-DBP) was measured in zebrafish embryos at 96 hours after fertilization. The fluorescence intensity was analyzed with ImageJ software. Animal work was conducted according to the guidelines of the American Physiological Society and was approved by Mount Desert Island Biological Laboratory (Salisbury Cove, ME) Institutional Animal Care and Use Committee (IACUC protocol #0804). All efforts were made to minimize the number of animals used and their suffering.

Transmission Electron Microscopy of Zebrafish

Larval zebrafish injected with capped mRNA were sampled at 120 h after fertilization and fixed in 1.5% glutaraldehyde/1%

paraformaldehyde, 70 mmol/L NaH_2PO_4, and 3% sucrose (pH 7.2). The embryos were washed three times in 0.2 mol/L cacodylate buffer and then postfixed in 1% osmium tetroxide for 1 h at room temperature. The specimens were rinsed with cacodylate buffer, dehydrated in a graded ethanol series, and infiltrated and embedded with Epon (Hard Plus Resin 812; Electron Microscopy Sciences, Hatfield, PA) according to the manufacturer's protocol. Thin-sections of 0.5 and 1 μm were generated with a Leica RM2165 rotary microtome and stained with 0.5% toluidine blue in a 1% sodium tetraborate solution. When the pronephros was identified on toluidine blue staining, ultrathin (80- to 100-nm-thick) sections of the kidney were cut and mounted on slot grids (Luxel, Friday Harbor, WA). The sections were stained with 2% uranyl acetate in distilled water and contrasted with lead citrate. Sections were viewed and photographed on a JEOL-1230 transmission electron microscope (Eching, Germany) and an attached charge-coupled device camera.

Clinical Renal Biopsy Samples

Renal tissue was obtained from the archives of the Hannover Medical School Department of Pathology. Paraffin-embedded specimens of normal kidney from nephrectomies performed for tumor and renal biopsy samples from adults with DN were included. The renal specimens were used in accordance with the ethical standards of the Hannover Medical School and with the Declaration of Helsinki of 1975, as revised in 1983. All patients consented at hospital admission to experiments on their anonymized archived tissue samples.

Statistics

The statistical analysis of data was performed with the table calculation program in Microsoft Excel or with GraphPad Prism software. Average and SEM were calculated for each datum. SEM is shown as an error bar. We used the unpaired Student *t* test to compare the results of each single test group. A P value of <0.05 was considered statistically significant.

RESULTS

Upregulation of Glomerular CIN85/RukL in Experimental and Human DN

High glucose is known to induce podocyte injury, yet the mechanisms remain largely elusive. To determine the regulatory effect of high glucose on podocyte slit diaphragm proteins, we examined the expression of CIN85/RukL, CD2AP, and nephrin in murine and human podocytes using Western blot analysis (Fig. 1). CIN85/RukL expression began to increase 24 h after high glucose stimulation ($P < 0.05$) and reached the highest level at 48 h ($P \leq 0.01$) in both cell lines (Fig. 1*A* and *C*). High glucose stimulation upregulated CIN85 expression by twofold but decreased the expression of CD2AP and nephrin. In contrast, treatment with mannitol as an osmotic control had no effect on the expression of these three proteins (Fig 1*B* and *D*). These results suggest that high glucose changes the expression balance of CD2AP and CIN85/RukL, leading to a downregulation of nephrin expression in murine and human podocytes.

SUMOylation of CIN85 Is Changed in Diabetes

To examine the alteration of CIN85/RukL expression and its posttranscriptional modification in experimental animal models of diabetes, 8-week-old C57BL/6J mice were injected with low-dose STZ to induce type 1 diabetes. At 16 weeks after diabetes induction, dual immunofluorescence staining of mouse kidney cortex sections with antibodies against CIN85 and SUMO-1 revealed a significantly upregulated expression of CIN85 in the glomeruli (Fig. 2*A*). Colocalization of CIN85 and SUMO-1 in C57BL/6J mice suggests that CIN85 is SUMOylated under normal conditions. SUMO-1 expression is distributed throughout the glomerulus under normal conditions but was predominantly restricted to the nucleus in diabetic glomeruli, indicating that CIN85 is released from SUMO-1 in diabetic glomeruli. To confirm these results, we performed immunoprecipitation of endogenous SUMO-1 and endogenous CIN85 from glomerular lysates isolated from CD2AP-knockout mice, wild-type mice, and diabetic mice (Fig. 2*D*). The immunoprecipitation demonstrated a reduced SUMOylation in diabetic mice; moreover, CD2AP expression was also significantly downregulated. Therefore, upregulated expression of CIN85 coincides with downregulation of CD2AP and reduced SUMOylation.

Dual immunofluorescence staining of mouse kidney cortex sections with antibody against CIN85 and nephrin revealed significantly upregulated expression of CIN85 in the glomeruli (Fig. 2*B*) and a reduction of nephrin expression. Decreased nephrin indicated a possible degradation of nephrin under diabetic conditions, which is associated with podocyte injury and proteinuria. Partial colocalization of CIN85 with nephrin indicates CIN85-positive podocytes. To investigate the CIN85 expression and localization in the glomeruli of patients with DN, immunoperoxidase staining was performed with human biopsy samples against antibodies recognizing CIN85 (Fig. 2*C*). CIN85 expression was barely detectable in glomeruli from normal control kidneys but was strongly upregulated in glomeruli from patients with DN ($n = 5$). Moreover, CIN85 staining localized specifically to human podocytes under disease conditions.

To confirm that colocalization of nephrin and CIN85 is due to their interaction, we performed coimmunoprecipitation of endogenous CIN85 with nephrin in C57BL/6J mice (Fig. 2*E*) and in cultured human podocytes (Fig. 2*F*). We detected a weak interaction of CIN85 with nephrin that was robustly induced when the mice were diabetic or the human podocytes were exposed to high glucose for 48 h. Collectively, these results suggest CIN85 may be a biological marker for podocyte injury in experimental and in human DN.

Absence of CIN85 Exon2 Preserves Expression of Nephrin Under Diabetic Conditions

$CIN85^{\Delta ex2}$ mice, which lack the two major CIN85 isoforms expressed in the kidney (CIN85-xl and CIN85/RukL) (23),

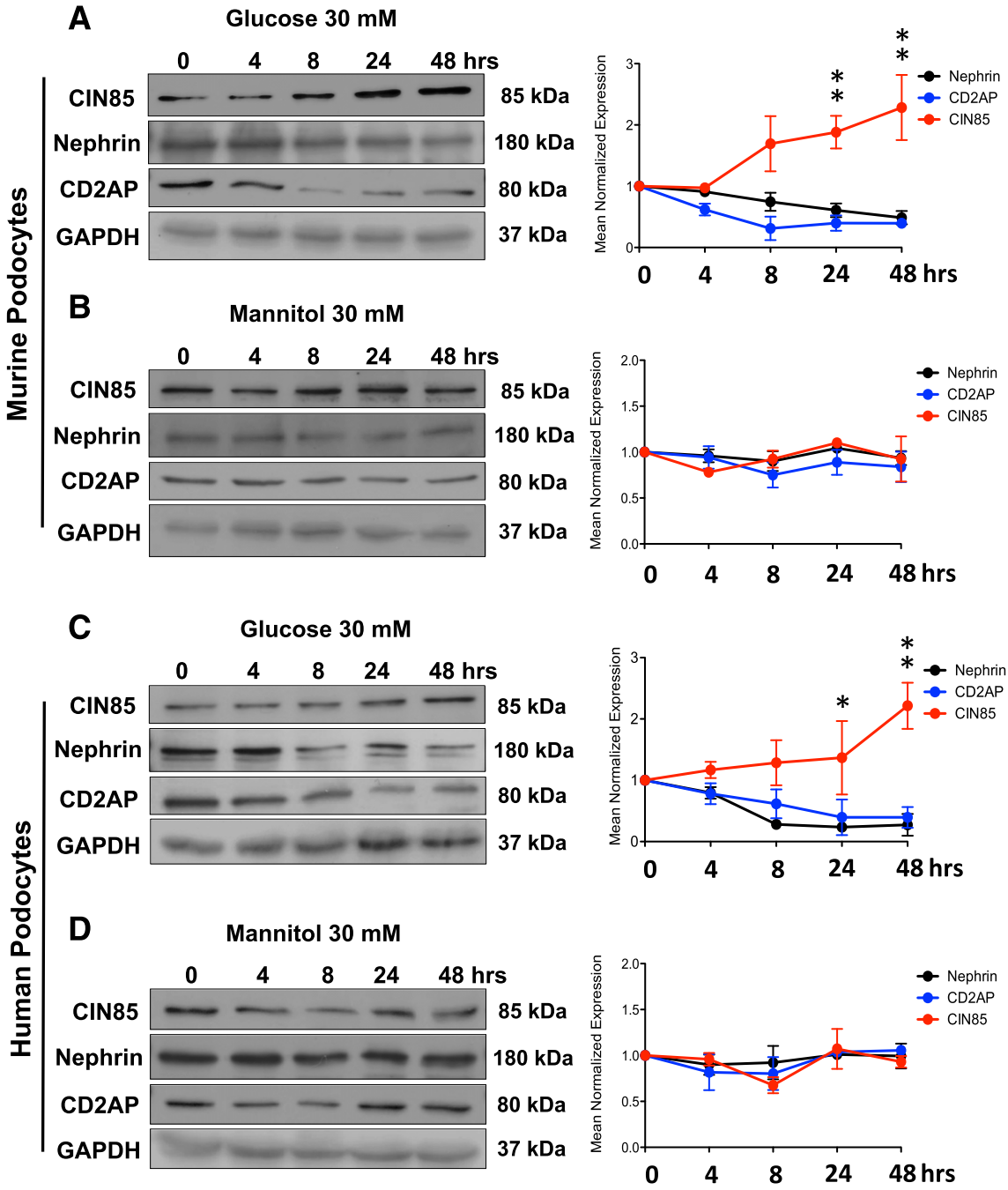

Figure 1—Time course of CIN85, CD2AP, and nephrin expression after glucose or mannitol stimulation in murine and human podocytes. Human and murine podocytes were exposed to 30 mmol/L high glucose or mannitol as osmotic control at the times indicated (0–48 h). Western blotting analysis depicts the expression of CIN85, CD2AP, and nephrin in murine podocytes (*A* and *B*) and human podocytes (*C* and *D*) (results are representative for three independent experiments). Expression level of CIN85, CD2AP, and nephrin were quantified by densitometry (right panels). High glucose augmented CIN85 expression in a time-dependent manner and reached the highest level at 48 h in murine (*A*) and human (*C*) podocytes, whereas a downregulated expression of CD2AP and nephrin was detected as early as 24 h after stimulation. Values are means ± SEM of three independent experiments expressed as percentage of control (0 h), where the ratio in control was defined as 100%. **P* ≤ 0.05, ***P* ≤ 0.01 vs. control (0 h) by unpaired *t* test.

were used to investigate the function of CIN85/RukL in DN. Homozygous CIN85$^{\Delta ex2}$ mice displayed no obvious renal phenotype abnormalities. C57BL/6J mice and CIN85$^{\Delta ex2}$ mice were injected with low-dose STZ to induce diabetes. At 16 weeks after STZ injection, we collected the spot urine and sacrificed the mice. Under diabetic conditions, nephrin was dramatically downregulated and lost much of its characteristic expression pattern. Strikingly, nephrin staining in sections from CIN85$^{\Delta ex2}$mice was preserved (Fig. 3*A*). When we examined

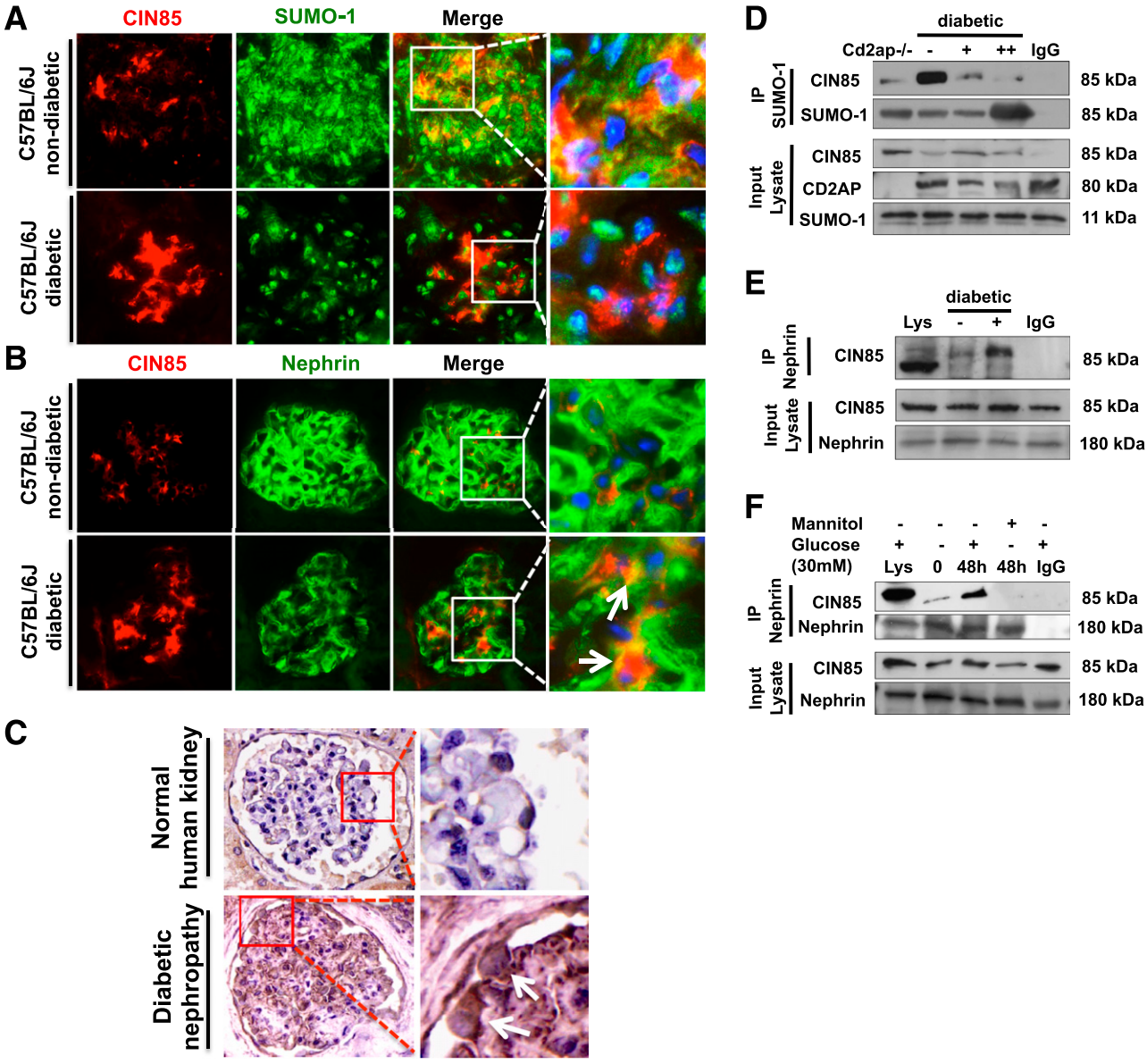

Figure 2—Increased glomerular CIN85 expression in mice and a patient with DN. *A*: CIN85 and SUMO-1 were visualized by dual immunofluorescence staining on cryosections of C57BL/6J and STZ-induced type 1 diabetic mice (n = 5 per group). In wild-type mice, colocalization of SUMO-1 and CIN85 indicate posttranscriptional modification of CIN85 by SUMOylation. In the renal cortex section of diabetic animals, SUMO-1 is predominantly localized in the nucleus, and colocalization with CIN85 is not detected. Original magnification ×63. *B*: Dual immunofluorescence staining with CIN85 and nephrin antibodies was performed on frozen kidney cortex sections of C57BL/6J and diabetic mice. In diabetic kidney sections, expression of CIN85 (red) was significantly increased, whereas the nephrin expression (green) was reduced. Colocalization of nephrin and CIN85 is depicted in yellow. CIN85 is partially colocalized with nephrin, indicating expression of CIN85 in projection of the slit diaphragm (white arrows). The pictures are representative for most of the glomeruli in the C57BL/6J and diabetic mice (n = 5 per group). Original magnification ×63. *C*: Representative immunoperoxidase staining for CIN85 in renal biopsy sections from a normal kidney (upper panels) and from a patient with DN (lower panels). The white arrows depict the distribution of CIN85 in podocytes. CIN85-positive podocytes could only be detected in the glomeruli of patients with DN (n = 5) but not in the glomeruli from normal control kidneys. Original magnification ×100. *D*: Downregulated SUMOylation of CIN85 in glomeruli of diabetic mice. Antibodies against SUMO-1 were used for immunoprecipitation (IP) experiments to detect interaction with glomerular lysates from CD2AP-knockout mice, nondiabetic C57BL/6J mice (−), and type 1 diabetic mice (+ indicates blood glucose level between 12 and 18 mmol/dL, ++ indicates blood glucose level above 18 mmol/dL). *E*: Nephrin and CIN85 are binding partners in vivo. Endogenous nephrin and CIN85 were precipitated using antibodies against nephrin and CIN85 on glomerular lysates isolated from C56BL/6J (−) and type 1 diabetic mice (+) (n = 5 per group). IgG antibody was used as a negative control, and whole glomerular lysate was used as input. *F*: Increased interaction between nephrin and CIN85 upon high glucose stimulation in human podocytes in vitro. The immunoprecipitation was performed with cell lysates of human podocytes with indicated treatment. Western blot analysis indicated a significantly enhanced association between nephrin and CIN85 48 h after high glucose treatment.

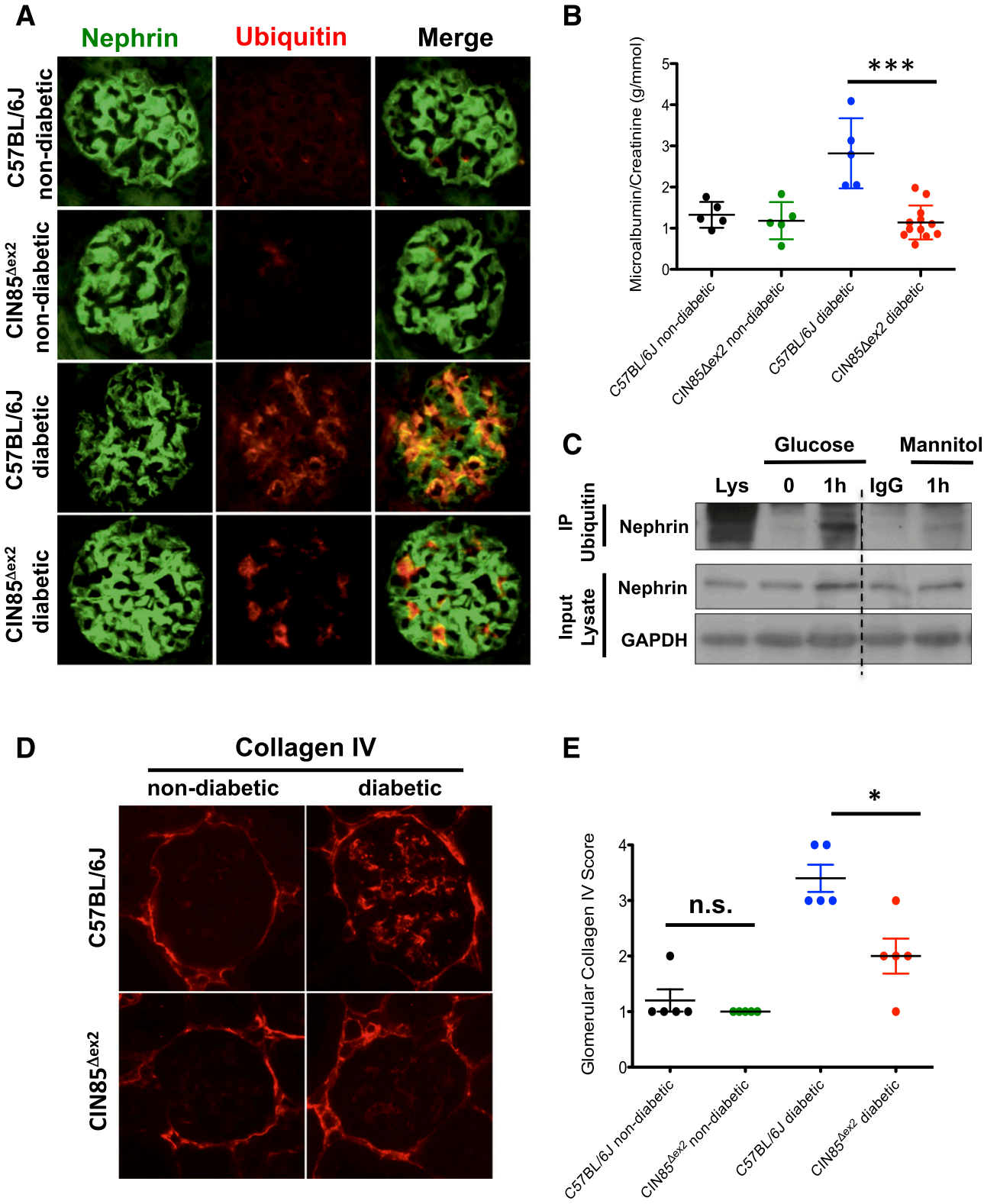

Figure 3—CIN85 exon2 deletion ameliorates proteinuria and glomerular matrix accumulation in diabetic mice. *A*: Immunofluorescence staining of mouse glomeruli using antibodies against nephrin (green) and ubiquitin (red). Ubiquitin partially colocalized with nephrin (yellow) in diabetic C57BL/6J mice. Ubiquitin-positive podocytes were increased in 16-week-old diabetic wild-type mice, whereas nephrin expression was downregulated. Nephrin expression was preserved in CIN85$^{\Delta ex2}$ mice, and substantially fewer ubiquitin-positive podocytes were detected under diabetic conditions compared with C57BL/6J diabetic mice. Original magnification ×60. *B*: Albuminuria in C57BL/6J mice was determined by analysis of spot urine samples of mice 16 weeks after low-dose STZ injection (n = 5 in first three conditions, n = 12 in CIN85$^{\Delta ex2}$ diabetic mice). The error bars show the mean ± SEM. ***$P \leq 0.001$ by unpaired t test. *C*: Ubiquitination assay using immunoprecipitation (IP) with antibody against nephrin and ubiquitin showed the ubiquitinated nephrin content increased 1 h after high glucose

the ubiquitin expression in the same the kidney sections, we found ubiquitin staining, which overlapped with nephrin staining, was increased in C57BL/6J diabetic mice, whereas little expression and overlap of ubiquitin and nephrin was detected in CIN85$^{\Delta ex2}$ diabetic mice (Fig. 3*A*). Remarkably, these results showed albuminuria was not induced in diabetic CIN85$^{\Delta ex2}$ mice compared with diabetic wild-type animals (Fig. 3*B*).

Because CIN85/RukL is a Cbl-interacting protein and Cbl directs ubiquitination of nephrin and mediates its endocytosis (24), we performed an ubiquitination assay using immunoprecipitation with endogenous nephrin in human podocytes and then performed immunoblotting for ubiquitin (Fig. 3*C*). Ubiquitinated nephrin was not detected at baseline or when treated with mannitol. High glucose treatment, however, resulted in a significant level of ubiquitinated nephrin with a major band above 180 kDa.

Collagen IV deposition in the glomeruli of diabetic C57BL/6J mice and diabetic CIN85$^{\Delta ex2}$ mice was also examined (Fig. 3*D*). The Bowman capsule consists of the meshwork of type IV collagen, indicating a comparable fluorescence intensity in the stainings, whereas collagen IV deposition within the glomerular tuft region and mesangial area was only detectable in diabetic C57BL/6J mice. Glomeruli were semiquantitively scored with a score of 1 to 4, depending on the intensity and distribution of collagen IV staining. Strikingly, hyperglycemia induced less collagen IV deposition and sclerosis lesions in CIN85$^{\Delta ex2}$ mice, resulting in a significantly lower glomerular collagen IV score. CIN85$^{\Delta ex2}$ diabetic mice received an average score of 2.5, whereas the diabetic C57BL/6J mice had an average score of 4 (Fig. 3*D* and *E*).

Nephrin Endocytosis Is Impaired by CIN85/CD2AP Balance

Because CIN85 has been described to bind Cbl and recruit ubiquitin and to be involved in endocytosis of several tyrosine kinase transmembrane receptors, we wanted to prove that CIN85/RukL is responsible for ubiquitination and endocytosis of nephrin under high glucose conditions. We demonstrated in our previous studies that CIN85/RukL is involved in nephrin internalization and that the binding of CIN85 to nephrin is affected by the protein balance of CD2AP. To investigate the effect of high glucose on nephrin endocytosis in different podocyte cell lines, we generated conditionally immortalized wild-type podocytes and CIN85$^{\Delta ex2}$ podocytes. The CIN85$^{\Delta ex2}$ cells had a normal appearance under the light microscope (Fig. 4*A*) and showed normal growth properties (data not shown). We confirm the absence of the CIN85/RukL isoform by Western blot analysis (Fig. 4*B*), which was in agreement with the observed loss of exon 2 confirmed by PCR (Fig. 4*C*). Because CIN85/RukL interacts with nephrin and is involved in its internalization, we performed endocytosis assays and quantified the endocytosis of nephrin in the absence of CIN85/RukL protein using an ELISA-based endocytosis assay, as previously described (18). We compared wild-type podocytes, CD2AP$^{-/-}$ podocytes, which have higher endogenously expressed CIN85/RukL levels (Fig. 4*B*), and CIN85$^{\Delta ex2}$ podocytes after 2 h of high glucose or mannitol exposure. High glucose treatment of CD2AP$^{-/-}$ podocytes for 2 h induced a nearly twofold increase in nephrin endocytosis compared with the wild-type podocytes; in contrast, CIN85$^{\Delta ex2}$ podocytes did not respond to high glucose stimulation (Fig. 4*D*). When we exposed the podocytes for 24 h, the nephrin endocytosis in wild-type podocytes was also significantly induced after exposure to high glucose levels, whereas nephrin on the surface of CIN85$^{\Delta ex2}$ podocytes was maintained even after high glucose stimulation for 24 h (Fig. 4*E*). Interestingly, the overexpression of CIN85 led to an increased endocytosis response in murine and human podocytes (Fig. 4*F* and *G*).

CIN85 Overexpression Resulted in a Severe Edema and Proteinuria in Zebrafish Embryos

The results described above suggest a protective effect of CIN85/RukL deletion on DN; therefore, we wanted to examine whether CIN85 overexpression results in disruption of the functional integrity of the glomerular filtration barrier in vivo. Zebrafish can be used as a comparative in vivo model because the ultrastructure of the zebrafish glomerulus is indistinguishable to the human glomerulus. The glomerular filtration barrier of zebrafish is also composed of three parts—the fenestrated glomerular endothelial cells, the intervening GBM, and the interdigitating foot processes of podocytes—and podocytic changes leading to effacement and proteinuria can be reproduced in zebrafish larvae as well (22).

Overexpression was accomplished by injection of murine CIN85-mRNA into 1- to 4-cell zebrafish embryos. CIN85 overexpression resulted in morphological changes in the embryos, such as shortened body length and pericardial and yolk sac edema, compared with wild-type or CD2AP mRNA–overexpressing zebrafish (Fig. 5*A*). The edema phenotype (P) was classified into four categories: P1, no edema; P2, mild edema; P3, severe edema; and P4, very severe edema (Fig. 5*B*). More than 95% of the wild-type and CD2AP-overexpressing fish had no edema (P1). However, with overexpression of CIN85, a low dose of 7.5 ng resulted in ~40% edema, whereas with higher doses of mRNA, edema developed in more than 50% of the larva.

stimulation. *D*: Representative images of glomeruli stained by immunofluorescence using anti-collagen IV. Collagen IV staining indicated increased matrix accumulation caused by diabetes. Original magnification ×60. *E*: Glomerular collagen IV expression in glomeruli from the indicated mice was semiquantitatively scored in a blinded fashion: score 1, very mild; score 2, mild; score 3, moderate; score 4, intense. The error bars show the mean ± SEM (n = 5 per condition). *$P \leq 0.05$; n.s., not statistically significant by unpaired t test.

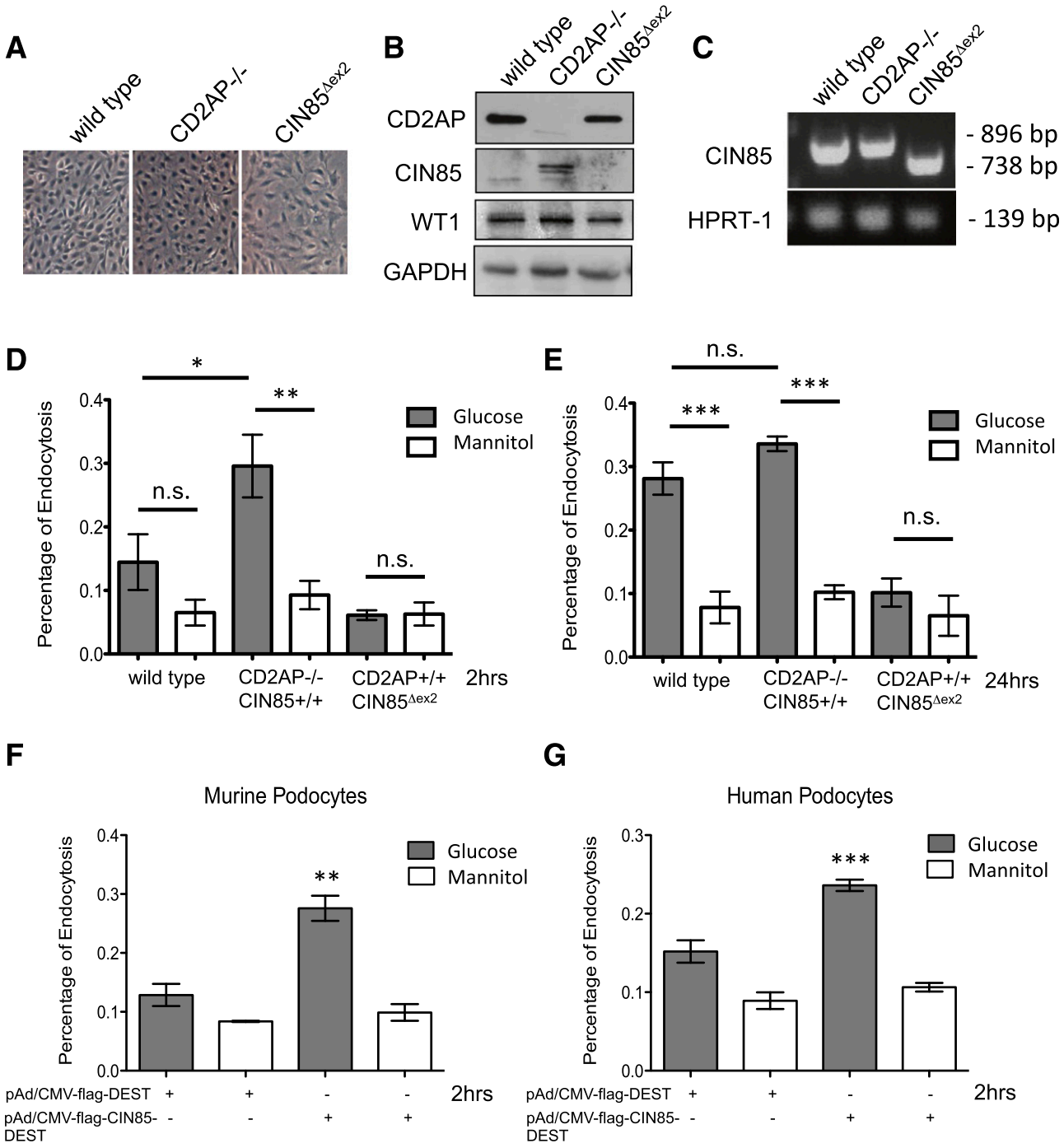

Figure 4—Impaired nephrin endocytosis in the absence of CIN85 after high glucose exposure. To perform the cell-based nephrin endocytosis assay, we generated conditional immortalized podocytes with CIN85 exon 2 deletion. *A*: Light microscopic morphology of cultured podocytes. CIN85$^{\Delta ex2}$ podocytes grown under nonpermissive conditions (37°C without γ-interferon) display similar morphology as wild-type and CD2AP$^{-/-}$ murine podocytes. Original magnification ×200. *B*: Western blot analysis showed a complete absence of full-length CIN85 in CIN85$^{\Delta ex2}$ podocytes. Full-length CIN85 was not detectable in wild-type podocytes but was seen in CD2AP-knockout podocytes. *C*: PCR analysis using primers against full-length CIN85 indicated the deletion of CIN85 exon 2 in murine podocytes. *D* and *E*: Nephrin molecules expressed on the surface of differentiated wild-type, CD2AP$^{-/-}$, and CIN85$^{\Delta ex2}$ murine podocytes were labeled with nephrin antibody, followed by incubation with high glucose and mannitol for 2 h and 24 h to induced endocytosis. *F* and *G*: An adenoviral system was used to transfect murine and human podocytes with CIN85-flag. Nephrin expressed on the cell surface was labeled with antibody against nephrin. The labeled podocytes were treated with high glucose for 2 h to induce internalization of nephrin. The error bars show the mean ± SEM (n = 5 per condition). *$P \leq 0.05$, **$P \leq 0.01$, ***$P \leq 0.001$; n.s., not statistically significant by unpaired t test.

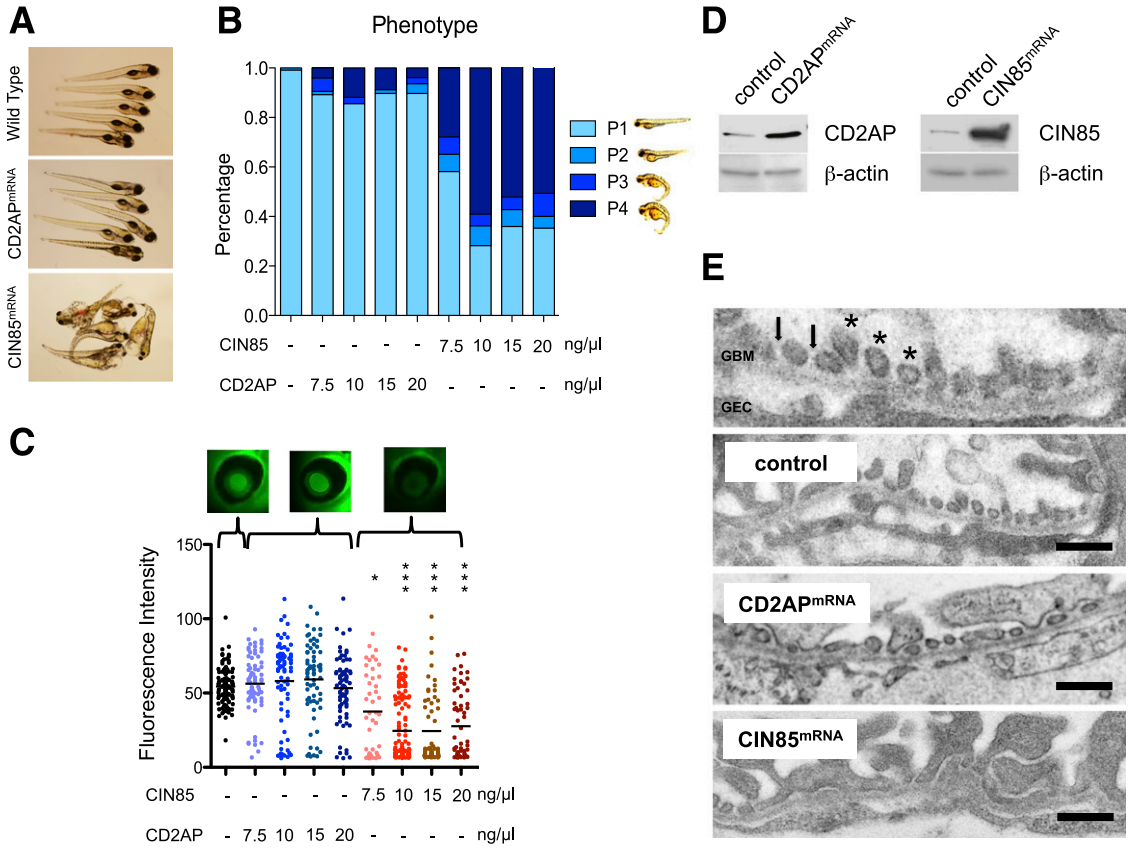

Figure 5—CIN85 expression impaired the integrity of the filtration barrier in zebrafish. Fertilized zebrafish eggs were injected at the 1- to 4-cell stage with murine CIN85 or CD2AP-capped mRNA in the indicated concentrations. *A*: Phenotype of zebrafish after CD2AP and CIN85 mRNA injection at 120 h after fertilization. The injected zebrafish larvae showed a very severe generalized edema and pericardial effusion. *B*: Categorization of zebrafish phenotype. At 120 h after fertilization, the phenotype of larvae was categorized into four groups: P1, no edema; P2, mild edema; P3, severe edema; and P4, very severe edema ($n > 50$ per condition). Compared with CD2AP mRNA–injected fish with 90% P1 phenotype, 7.5 ng CIN85 mRNA induced edema in ~40% of embryos, and 10 ng CIN85 mRNA led to edema in >60% of embryos ($n > 50$ per condition). *C*: Fluorescent images of the retinal vessel plexus. Bar graph presenting fluorescence intensity of eGFP-DBP in the fish eye under indicated conditions was analyzed by ImageJ software. The CIN85 overexpression induced proteinuria showed in a dose-dependent manner. At least 50 animals were measured for each condition. The error bars show the mean ± SEM. $^{*}P \leq 0.05$, $^{***}P \leq 0.001$ by unpaired *t* test. *D*: Expression of CD2AP and CIN85 capped-mRNA was determined using Western blot analysis. *E*: Ultrastructural analysis of the zebrafish glomerular structures using transmission electron microscopy. Under normal conditions, the secondary foot process of podocytes can be visualized (*). The black arrows depict slit diaphragms. GEC, glomerular endothelial cells. Scale bars: 500 nm. Control fish and fish injected with CD2AP mRNA displayed normal foot processes, whereas in zebrafish injected with CIN85 mRNA, podocyte foot processes and slit diaphragms are lost (effacement).

We next examined proteinuria in mRNA-overexpressing zebrafish. The integrity of the glomerular filtration barrier of zebrafish is assessed by measuring the retention or loss of transgenically overexpressed eGFP-DBP in the circulation of the zebrafish embryos, as previously described (21,22). A decrease in circulating eGFP-DBP is usually accompanied by foot process effacement and the appearance of eGFP-DBP–mediated fluorescence in the tank water, indicative of a compromised glomerular filtration barrier in the manipulated fish. Compared with wild-type fish, fish overexpressing CIN85 exhibited a significant and dose-dependent decrease in circulating eGFP-DBP (Fig. 5*C*). Expression of murine CD2AP and CIN85/RukL protein was confirmed in zebrafish embryos by Western blotting (Fig. 5*D*). To confirm the phenotype is caused by disruption of the glomerular filter, the fish embryos were embedded, and ultrathin sections were examined by electron microscopy (Fig. 5*E*). The glomerulus of wild-type and CD2AP-overexpressing fish showed well-structured podocyte foot processes with cross sections of interdigitating foot processes and intact slit diaphragms. However, CIN85 overexpression resulted in effacement of foot processes, indicating a detrimental effect of CIN85/RukL expression on podocyte integrity. These results explain the decreased fluorescence in the circulation of the fish with CIN85/RukL overexpression, which indicates a direct effect of CIN85 expression on the podocyte phenotype in vivo.

DISCUSSION

We previously demonstrated that the paralogs CD2AP and CIN85/RukL are functionally distinct in podocytes.

Both proteins bind to the slit diaphragm protein nephrin, but whereas the interaction to CD2AP seems to stabilize the slit diaphragm complex, the interaction of nephrin and CIN85/RukL leads to ubiquitination and internalization of nephrin (18). We also previously described that the expression of CD2AP determines the expression level of free CIN85/RukL in podocytes. In the presence of CD2AP, CIN85/RukL is posttranslationally modified by SUMO, and this modification prevents its binding to nephrin (19). Although our previous studies were mainly performed under conditions of CD2AP knockout, which is an extremely rare genetic defect in humans, we present here for the first time evidence that this pathway might be relevant to glomerular changes observed in diabetes. We can demonstrate a downregulation of CD2AP in murine and human podocytes after exposure to high glucose. This is well in line with the observation of Ha et al. (25) who observed a phosphatidyl inositol 3-kinase–dependent mechanism of CD2AP expression after high glucose exposure. At the same time, we detect a significantly reduced nephrin expression as a consequence of high glucose exposure. This is consistent with previous observations, by us and others, that high glucose exposure leads to nephrin endocytosis in podocytes (26,27). How nephrin specifies clathrin-mediated endocytosis or raft-mediated endocytosis pathways and how these trafficking routes are coordinated with the signaling function is still unclear. In vitro experiments with podocyte cell lines suggested that nephrin can undergo both clathrin- and raft-mediated endocytosis (28). We hypothesize here that the observed downregulation of CD2AP has a secondary effect on the expression of full-length CIN85/RukL in podocytes and that this contributes to a continuous internalization of nephrin from the podocyte surface in diabetes (Fig. 6). Our hypothesis is supported by the following evidence.

Firstly, we document a parallel downregulation of CD2AP and nephrin, which inversely correlates with the upregulated expression of CIN85 in two different cell lines, murine and human podocytes, after high glucose treatment in culture.

Secondly, we demonstrate an upregulation of glomerular CIN85 expression in murine and human diabetes with a strong overlap in nephrin expression and a clear localization to podocytes. In addition, we detected a glucose-inducible interaction of CIN85 and nephrin in vitro. Our work provides the first study of mammalian diabetes in which loss of CIN85 is analyzed in vivo. The CIN85-deficient mice were generated by removing the two full-length isoforms CIN85-xl and CIN85/RukL by deletion of exon 2. In the absence of these two protein isoforms, nephrin expression is preserved in the glomerulus and proteinuria is significantly reduced. We furthermore defined a glucose-induced ubiquitination response of nephrin, which explains the endocytosis and, presumably, the degradation of nephrin. Although monoubiquitination of CIN85/RukL is thought to regulate its interaction with E3 ubiquitin ligase c-Cbl and to target this adaptor together with activated transmembrane

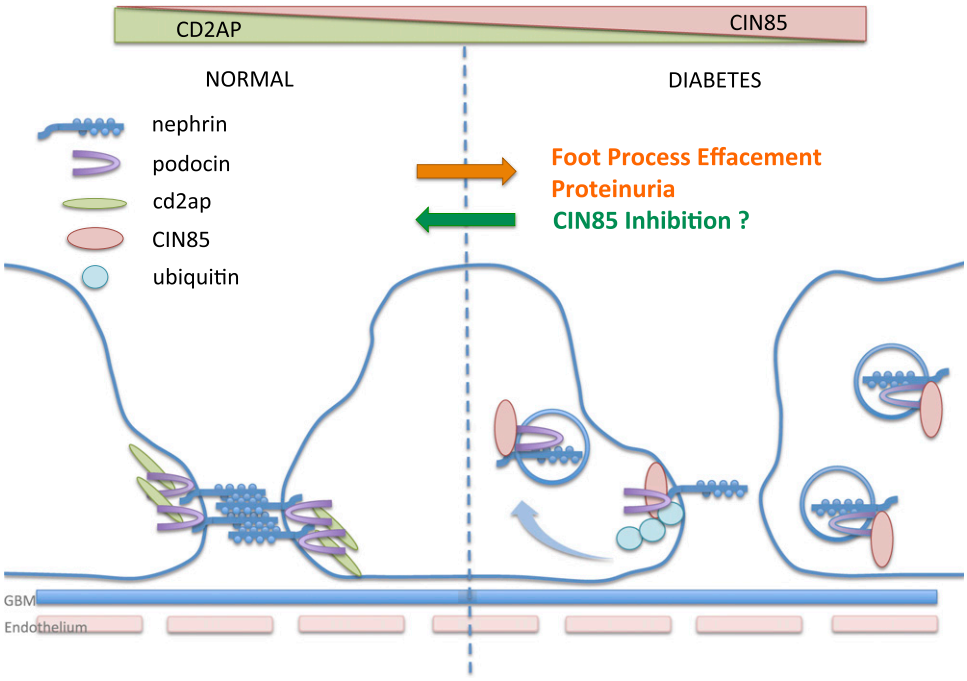

Figure 6—Schema of CIN85-induced nephrin endocytosis under diabetic conditions. In the presence of CD2AP, the complexes on the slit diaphragm are stabilized. Diabetes/high glucose downregulates CD2AP expression, which leads to increased full-length CIN85 expression. CIN85 is required for cbl-mediated ubiquitination and trafficking of nephrin. Nephrin endocytosis leads to proteinuria. Deletion of CIN85 preserves the nephrin expression and ameliorates the proteinuria and glomerular matrix accumulation.

receptors for proteasomal degradation (29), separate studies suggest that ubiquitination alone is not sufficient to target CIN85/RukL to proteasomes or to lysosomes (30). Therefore, it is conceivable that additional steps follow that induce proteasomal degradation of nephrin. It is tempting to speculate that the monoubiquitination of nephrin is reversible and that other posttranslational pathways, such as SUMO, could orchestrate nephrin recycling back to the podocyte surface as we postulated earlier (19). However, recycling is unlikely under sustained diabetic conditions.

Thirdly, we provide additional in vitro evidence that the CIN85/RukL levels in podocytes define the level of glucose-induced nephrin endocytosis. Clearly CD2AP-knockout podocytes with an upregulated endogenous CIN85/RukL level have the strongest endocytosis response after high glucose stimulation. Already 2 h after high glucose stimulation, we can detect a significant increase in nephrin endocytosis. At that time, wild-type cells do not yet show a significant endocytosis response. When we examine endocytosis 24 h after high glucose stimulation, we can detect significant nephrin endocytosis also in wild-type cells. This is consistent with the upregulated concentration of CIN85/RukL in wild-type cells detectable 24 h after high glucose exposure. In contrast, CIN85$^{\Delta ex2}$ podocytes that do not express CIN85/RukL do not show a significant nephrin endocytosis response after 2 h or after 24 h, indicating that CIN85/RukL is indispensable for the glucose-induced endocytosis complex of slit diaphragm proteins. However, we hypothesize that nephrin is not only the target of CIN85 but also may be a trigger for endocytosis of several transmembrane receptors or structure proteins. The endocytosis of nephrin seems to have severe consequences for the podocytes under diabetic conditions. In addition, nephrin is most likely internalized in a complex with other slit diaphragm proteins that do not directly bind to CIN85.

Because we had previously observed in vitro that the artificial overexpression of CIN85/RukL could induce an increased endocytosis of overexpressed nephrin in HEK cells (18), we wanted to test whether overexpression of CIN85/RukL could also induce proteinuria in vivo. We used the zebrafish vertebrate system to accomplish this and induced expression of CIN85/RukL by injection of in vitro transcribed murine mRNA. As a control, we injected CD2AP mRNA at the same concentration. The amino acid sequence identity of zebrafish and murine CD2AP and CIN85 is 46.8% and 70.4% (71% and 86.1% similarity), respectively. Interestingly, overexpression of CIN85/RukL induced a severe edema phenotype, significant proteinuria, and foot process effacement in the injected zebrafish embryos, whereas injection of similar concentrations of CD2AP mRNA had no detrimental effect on foot process architecture. The overexpression of CIN85/RukL alone leads to a breakdown of podocyte foot process architecture, presumably through endocytosis of slit diaphragm components.

This is the first report discussing the importance of CIN85/RukL expression and the associated ubiquitination of slit diaphragm components in the context of a nongenetic disease. The expression under high glucose conditions is clearly dependent on expression levels of CD2AP. Interestingly, a recent study reported that CD2AP variants may be associated with susceptibility to end-stage renal disease in patients with type 1 diabetes (31). Our results could serve as a first mechanistic insight of how gene variants of CD2AP could contribute to disease progression in diabetic kidney disease. Thus, CIN85/RukL could serve as a novel biomarker indicating diabetes/high glucose–induced stress in podocytes.

Acknowledgments. The CIN85$^{\Delta ex2}$ mice were gifts from I.D. Tg(L-FABP:DBP-EGFP) and Tg(*l*-fabp:DBP-EGFP) zebrafish were gifts from J. Xie and B. Anand-Apte, Cleveland Clinic, Cleveland, OH.

Funding. This work was supported by the Deutsche Forschungsgemeinschaft (SCHI587/3,4,6).

Duality of Interest. No potential conflicts of interest relevant to this article were reported.

Author Contributions. B.T. analyzed the data. B.T., P.S., J.M.-D., H.S., L.S., and I.T. performed the research. B.T., I.D., H.H., and M.S. designed the research. B.T., P.S., and M.S. wrote the manuscript. B.T. and M.S. are the guarantors of this work and, as such, had full access to all the data in the study and take responsibility for the integrity of the data and the accuracy of the data analysis.

References

1. Fioretto P, Mauer M. Histopathology of diabetic nephropathy. Semin Nephrol 2007;27:195–207
2. Jefferson JA, Shankland SJ, Pichler RH. Proteinuria in diabetic kidney disease: a mechanistic viewpoint. Kidney Int 2008;74:22–36
3. Susztak K, Raff AC, Schiffer M, Böttinger EP. Glucose-induced reactive oxygen species cause apoptosis of podocytes and podocyte depletion at the onset of diabetic nephropathy. Diabetes 2006;55:225–233
4. Stieger N, Worthmann K, Teng B, et al. Impact of high glucose and transforming growth factor-β on bioenergetic profiles in podocytes. Metabolism 2012;61:1073–1086
5. Teng B, Duong M, Tossidou I, Yu X, Schiffer M. Role of protein kinase C in podocytes and development of glomerular damage in diabetic nephropathy. Front Endocrinol (Lausanne) 2014;5:179
6. Benzing T. Signaling at the slit diaphragm. J Am Soc Nephrol 2004;15:1382–1391
7. Diez-Sampedro A, Lenz O, Fornoni A. Podocytopathy in diabetes: a metabolic and endocrine disorder. Am J Kidney Dis 2011;58:637–646
8. Ruotsalainen V, Patrakka J, Tissari P, et al. Role of nephrin in cell junction formation in human nephrogenesis. Am J Pathol 2000;157:1905–1916
9. Huber TB, Kottgen M, Schilling B, Walz G, Benzing T. Interaction with podocin facilitates nephrin signaling. J Biol Chem 2001;276:41543–41546
10. Schiffer M, Bitzer M, Roberts IS, et al. Apoptosis in podocytes induced by TGF-beta and Smad7. J Clin Invest 2001;108:807–816
11. Kowanetz K, Husnjak K, Höller D, et al. CIN85 associates with multiple effectors controlling intracellular trafficking of epidermal growth factor receptors. Mol Biol Cell 2004;15:3155–3166
12. Szymkiewicz I, Kowanetz K, Soubeyran P, Dinarina A, Lipkowitz S, Dikic I. CIN85 participates in Cbl-b-mediated down-regulation of receptor tyrosine kinases. J Biol Chem 2002;277:39666–39672
13. Dikic I. CIN85/CMS family of adaptor molecules. FEBS Lett 2002;529:110–115
14. Buchman VL, Luke C, Borthwick EB, Gout I, Ninkina N. Organization of the mouse Ruk locus and expression of isoforms in mouse tissues. Gene 2002;295:13–17

15. Finniss S, Movsisyan A, Billecke C, et al. Studying protein isoforms of the adaptor SETA/CIN85/Ruk with monoclonal antibodies. Biochem Biophys Res Commun 2004;325:174–182
16. Urbé S. Ubiquitin and endocytic protein sorting. Essays Biochem 2005;41: 81–98
17. Swaminathan G, Tsygankov AY. The Cbl family proteins: ring leaders in regulation of cell signaling. J Cell Physiol 2006;209:21–43
18. Tossidou I, Teng B, Drobot L, et al. CIN85/RukL is a novel binding partner of nephrin and podocin and mediates slit diaphragm turnover in podocytes. J Biol Chem 2010;285:25285–25295
19. Tossidou I, Himmelseher E, Teng B, Haller H, Schiffer M. SUMOylation determines turnover and localization of nephrin at the plasma membrane. Kidney Int 2014;86:1161–1173
20. Mundel P, Reiser J. New aspects of podocyte cell biology. Kidney Blood Press Res 1997;20:173–176
21. Hanke N, King BL, Vaske B, Haller H, Schiffer M. A fluorescence-based assay for proteinuria screening in larval zebrafish (Danio rerio). Zebrafish 2015; 12:372–376
22. Hanke N, Staggs L, Schroder P, et al. "Zebrafishing" for novel genes relevant to the glomerular filtration barrier. Biomed Res Int 2013;2013:658270
23. Shimokawa N, Haglund K, Hölter SM, et al. CIN85 regulates dopamine receptor endocytosis and governs behaviour in mice. EMBO J 2010;29:2421–2432
24. Meyer-Schwesinger C, Meyer TN, Münster S, et al. A new role for the neuronal ubiquitin C-terminal hydrolase-L1 (UCH-L1) in podocyte process formation and podocyte injury in human glomerulopathies. J Pathol 2009;217:452–464
25. Ha TS, Hong EJ, Han GD. Diabetic conditions downregulate the expression of CD2AP in podocytes via PI3-K/Akt signalling. Diabetes Metab Res Rev 2015; 31:50–60
26. Tossidou I, Teng B, Menne J, et al. Podocytic PKC-alpha is regulated in murine and human diabetes and mediates nephrin endocytosis. PLoS One 2010; 5:e10185
27. Quack I, Woznowski M, Potthoff SA, et al. PKC alpha mediates beta-arrestin2-dependent nephrin endocytosis in hyperglycemia. J Biol Chem 2011; 286:12959–12970
28. Qin XS, Tsukaguchi H, Shono A, Yamamoto A, Kurihara H, Doi T. Phosphorylation of nephrin triggers its internalization by raft-mediated endocytosis. J Am Soc Nephrol 2009;20:2534–2545
29. Haglund K, Shimokawa N, Szymkiewicz I, Dikic I. Cbl-directed monoubiquitination of CIN85 is involved in regulation of ligand-induced degradation of EGF receptors. Proc Natl Acad Sci U S A 2002;99:12191–12196
30. Verdier F, Valovka T, Zhyvoloup A, et al. Ruk is ubiquitinated but not degraded by the proteasome. Eur J Biochem 2002;269:3402–3408
31. Hyvönen ME, Ihalmo P, Sandholm N, et al. CD2AP is associated with end-stage renal disease in patients with type 1 diabetes. Acta Diabetol 2013;50:887–897